Talanta 81 (2010) 162–166

Contents lists available at ScienceDirect

Talanta

journal homepage: www.elsevier.com/locate/talanta

Preparation and characteristics of protein molecularly imprinted membranes on the surface of multiwalled carbon nanotubes

Maosheng Zhang[a], Jiarong Huang[a], Ping Yu[c], Xi Chen[b,*]

[a] Department of Chemistry and Environmental Science, Fujian Province University Key Laboratory of Analytical Science, Zhangzhou Normal University, Zhangzhou 363000, China
[b] State Key Laboratory of Marine Environmental Science, Xiamen University, Xiamen 361005, China
[c] Fujian Research Institute of Metric Science, Fuzhou 350003, China

ARTICLE INFO

Article history:
Received 20 August 2009
Received in revised form
19 November 2009
Accepted 23 November 2009
Available online 2 December 2009

Keywords:
Molecular imprinting technology
Multiwalled carbon nanotubes
Bovine serum albumin
Protein

ABSTRACT

A novel protein molecularly imprinted membrane (PMIM) was synthesized on the surface of multiwalled carbon nanotubes (MWNTs) through a surface molecular imprinting technique by using bovine serum albumin (BSA) as the template molecule, acrylamide (AAm) as the functional monomer, N,N′-methylenebisacrylamide (NNMBA) as the cross-linker and ammonium persulphate [$(NH_4)_2S_2O_8$] as the initiator. The amounts of raw materials were optimized in this paper and the suitable amount is 0.1 g of CNTs, 0.02 g of BSA, 0.24 g of AAm, 0.1 g of MBA and 0.025 mg of $(NH_4)_2S_2O_8$. The selective recognition ability of PMIM/MWNTs was evaluated using adsorption experiments. Maximum adsorption capacity was 5.53 μg/mg PMIM/MWNTs and a saturation value was achieved at a BSA concentration of 0.2 mg/mL. The selectivity adsorption experiments showed that the PMIM/MWNTs also had higher adsorption capacities for BSA than for such molecules, as HSA, HB, pepsin and HRP. The PMIM/MWNTs displayed a 2.6-fold increase in affinity to BSA compared to the nPMIM/MWNTs. The PMIM/MWNTs, on the other hand, did not exhibit any significant change in affinity to other molecules compared to the nPMIM/MWNTs. In the experiment, the characteristics of the PMIM/MWNTs were analyzed using infrared spectroscopy and their configurations were observed using scanning electron microscopy.

1. Introduction

Molecularly imprinted polymers (MIPs) are prepared by copolymerizing a monomer with a cross-linker in the presence of a template molecule. After polymerization, the template is removed from the porous network by washing, leaving cavities in the polymeric matrix that are complementary in size, shape, and chemical functionality to the template. Thus, MIPs can rebind selectively with the template under certain experimental conditions. MIPs are very attractive because of their unique pre-determinative characteristics, and their specific and practical abilities for template molecule recognition. In 1993 the first molecularly imprinted sorbent assay was reported in which polymers imprinted with either theophylline or diazepam replaced antibodies in competitive immunoassay-like experiments [1]. To date, MIPs have been developed for the recognition of target molecules, such as drugs [2], small analytes [3], peptides [4] and proteins [5–8], and they have already been used successfully as biosensors, in immunoassays, as separation media, and as affinity supports for screening libraries of bioactive compounds.

The effectiveness of molecular imprinting in the polymeric matrix is greatly dependent on the bond nature of the template–monomer complex [9,10], the form of imprinted materials [11,12], and the rigidity of the polymeric matrix. In principle, a main challenge to the traditional imprinted materials is that the removal of original templates located at the interior area of bulk materials is very difficult due to the high cross-linking nature of imprinted materials [13–15], reducing the capacity of rebinding target analyte. Furthermore, if the generated cavities are not at the surface or in the proximity of the materials' surface, the high resistance to mass transfer will still hinder target species from accessing the deep imprinted cavities, thus reducing the kinetics of binding target analyte. Recently, the development of nanotechnology has offered an opportunity to solve these problems because of the unique characteristics of nanomaterials. So, several research groups have attempted by preparing MIPs as nanomaterials thus as nanowires, nanocapsule, nanospheres and nanofibers [16–23]. In these studies, the molecular imprinting at the nanostructures with high surface-to-volume ratio can provide more complete removal of templates, better site accessibility, lower mass-transfer

* Corresponding author. Tel.: +86 592 218 4530; fax: +86 592 218 6401.
E-mail address: xichen@xmu.edu.cn (X. Chen).

0039-9140/$ – see front matter © 2009 Elsevier B.V. All rights reserved.
doi:10.1016/j.talanta.2009.11.052

resistance, and well-defined materials' shape. However, the drawback whereby the templates located at the interior of materials could not be avoided fully in these studies [18,21]. Addressing these problems is usually attempted by controlling templates to locate at the surface of nanomaterials. So, some researches have begun to explore surface imprinting or alternative approaches for developing molecularly imprinted nanomaterials. Wang and co-workers have prepared a novel composite of multiwalled carbon nanotubes and molecularly imprinted polymers by using dopamine as a template molecule [24]. Zhang et al. reported the molecular imprinting at the walls of highly uniform silica nanotubes for the recognition of 2,4,6-trinitrotoluene [25]. These studies all used low molecular weight compounds as template molecules, comparatively few reports describe imprinting macromolecule materials, such as protein. Therefore, we attempted to find a new preparation method for MIPs combining both surface molecular imprinting technology and nanotechnology, and covering multiwalled carbon nanotubes (MWNTs) with a protein molecularly imprinted membrane (PMIM) in order to make protein molecularly imprinted membrane multiwalled carbon nanotubes (PMIM/MWNTs).

In this study, new protein molecularly imprinted membrane multiwalled carbon nanotubes (PMIM/MWNTs) were synthesized using MIT on the surface of MWNTs, using bovine serum albumin (BSA) as the template molecule, acrylamide (AAm) as the functional monomer, N,N′-methylenebisacrylamide (NNMBA) as the cross-linker and ammonium persulphate [$(NH_4)_2S_2O_8$] as the initiator. Then, the selective recognition of PMIM/MWNTs was evaluated using adsorption experiments. Compared to non-imprinted membrane multiwalled carbon nanotubes (nPMIM/MWNTs), the PMIM/MWNTs exhibited excellent recognition and selective ability to BSA. The large protein molecule binding capacity of the PMIM/MWNTs was obtained due to the large surface area of the MWNTs and the protein imprinted sites located on their surfaces. In this study, the components of PMIM/MWNTs were analyzed using infrared spectroscopy and their configurations were observed using scanning electron microscopy (SEM).

2. Experimental

2.1. Reagents and materials

Multiwall CNTs (diam. 40–60 nm, length 5–15 μm) were purchased from the Shenzhen Nanotech Port Co., Ltd. (Shenzhen, China). BSA (molecular weight (MW) 64 kDa), human serum albumin (HSA, MW 66 kDa), hemoglobin bovine blood (HB, MW 67 kDa), horseradish peroxidase (HRP, MW 40 kDa) and pepsin were all obtained from the Sigma Chemical Company (St. Louis, MO, USA). AAm and NNMBA were purchased from the Sinopharm Chemical Reagent Co., Ltd. (Shanghai, China). All other chemicals were of analytical grade and used as received. Pure water from a Simplicity Personal Ultrapure Water System (Millipore, USA) was used to prepare all buffers and other solutions.

2.2. Instrumentation

UV–vis spectra were obtained using a DU-7400 UV-Vis spectrophotometer (Beckman, USA). SEM observations of the surface of PMIM/MWNTs were made using an LEO-1530 SEM (Oxford Co., UK) with an accelerating voltage at 20 kV. Fourier transform infrared spectroscopy (FTIR) measurements were used to analyze the chemical bonding, and FTIR spectra were recorded using an FT-IR7400SX spectrometer (Thermo Nicolet Co., USA).

2.3. Preprocessing of MWNTs

Similar to the approach of Liu et al. [26], received-MWNTs were further cut into short pipes by chemical oxidation in a mixture of concentrated sulfuric and nitric acids (3:1, 98% and 70%, respectively) under ultrasonication at 70 °C for 4 h. The reaction mixture was then diluted with water and allowed to stand overnight for precipitation. The supernatant was decanted, and the remains were diluted with pure water and filtered with a 0.22 μm pore diameter polytetrafluoroethylene (PTFE) membrane (Gelman). Solid MWNTs were obtained by washing the remains on the PTFE filter with pure water until the filtrate pH became nearly neutral. The MWNTs were dried at 80 °C in a vacuum oven, and then powdered in a mortar.

2.4. Preparation of PMIM/MWNTs

The required amount of BSA and AAm were dissolved in 5 mL of phosphate buffer solution (PBS, pH 6.80) and ultrasonicated for 0.5 h to form the first aqueous phase. The required amount of NNMBA and 0.15 mg/mL of $(NH_4)_2S_2O_8$ were slowly added to the first aqueous phase. Subsequently, 0.1 g of processed MWNTs was added into the second aqueous phase and ultrasonicated for 0.5 h. The mixture was incubated overnight at 4 °C. Following incubation, centrifugation was performed at 10,000 rpm for 30 min and the upper solution removed. Upon completion, the polymer was washed five times, each with 10 mL of PBS, until no BSA was found in the solution after centrifugation. nPMIM/MWNTs were prepared in the same way but without the addition of the template to the first aqueous phase.

2.5. Adsorption experiments of BSA on PMIM/MWNTs or nPMIM/MWNTs

To investigate the adsorption dynamics of BSA on PMIM/MWNTs or nPMIM/MWNTs, the required amount of PMIM/MWNTs or nPMIM/MWNTs was put into a 10 mL conical flask and mixed with 3 mL 100 μg/mL (C_0) BSA standard solution. The mixture was vibrated on a vibrator for 3 h at a frequency of 150 r/min, and then centrifuged at 10,000 rpm for 30 min. After adsorption, the concentration of BSA in the upper solution was determined using the Bradford assay at a wavelength of 595 nm. The adsorbance (Q) was calculated based on the difference in BSA concentration before and after the adsorption in a constant volume of aqueous solution and a constant weight of the PMIM/MWNTs or nPMIM/MWNTs, according to:

$$\text{adsorbance } Q = \frac{(C_0 - C)V}{M}$$

where C_0 is the initial BSA concentration (mg/mL), C is the BSA concentration after adsorption, V is the volume of BSA solution (mL), and M is the weight of the PMIM/MWNTs or nPMIM/MWNTs (g).

3. Results and discussion

3.1. Effects of the amount of monomer and cross-linker

Having suitable amounts of monomer and cross-linker plays a key role affecting the characteristics of PMIM/MWNTs. To achieve a good recognition characteristic, a series of PMIM/MWNTs with different amounts of AAm and NNMBA was prepared, and then adsorption experiments were carried out following the description in Section 2. As shown in Table 1, it is obvious that the adsorbance Q increased with the increase in the amount of monomer or cross-linker, due to the effect of the increase in the recognition cavity amount on the MWNTs. However, agglomeration of the raw materials would happen if excessive amounts of monomer and cross-linker were used in the preparation. Our experimental results revealed that 0.24 g of AAm and 0.10 g of NNMBA were suitable in this work.

Table 1
Effect of the amount of raw materials on adsorption amount of PMIM/MWNTs.

No.	MWNTs (g)	Amount of raw materials				Adsorbance Q (μg/mg)
		BSA (g)	AAm (g)	NNMBA (g)	$(NH_4)_2SO_4$ (mg)	
1	0.1	0.02	0.01	0.01	0.025	1.46
2	0.1	0.02	0.05	0.03	0.025	1.52
3	0.1	0.02	0.12	0.05	0.025	2.13
4	0.1	0.02	0.24	0.10	0.025	3.96
5	0.1	0.02	0.36	0.15	0.025	~
6	0.1	0.02	0.48	0.2	0.025	~

~ The adsorption experiments were not carried out because of agglomeration of PMIM/MWNTs.

3.2. Influence of template molecule amount

Since the cavities formed in PMIM/MWNTs depended on the template molecule content, further experiments were performed to determine the optimum amount of template molecule. To evaluate the influence of BSA amount, 0.1 g of MWNTs, 0.24 g of AAm, 0.1 g of NNMBA and different amounts of BSA (0, 0.005, 0.01, 0.02, 0.05 and 0.1 g) were selected in the preparation of PMIM/MWNTs. The results of the adsorption experiments are given in Fig. 1. It is evident from the graph that the adsorbance *Q* increased with rise of template molecule content when the amount of BSA was below 0.02 g, since the increase in template molecule content led to an increase in the number of recognition cavities on the surface of the PMIM/MWNTs. When the amount of BSA was above 0.02 g, no dramatic increase in the adsorbance *Q* could be obtained with any additional template molecule content. The interaction and impact between template molecules at a higher concentration of BSA in the process of PMIM/MWNTs synthesis caused a decrease in the valid recognition cavities. Therefore, 0.02 g of BSA was selected in this work.

3.3. FTIR spectra of PMIM/MWNTs

FTIR spectra were applied to characterize the structural changes of MWNTs and PMIM/MWNTs (Fig. 2). Compared with the IR spectrum of received-MWNTs as shown in Fig. 2-1, new peaks at 2909 and 2848 cm^{-1} for the acid processed MWNTs can be found in Fig. 2-2, which corresponded to the contributions of $-CH_3$ and $=CH_2$ on the surfaces of the MWNTs. The stronger peaks at 3441 and 1623 cm^{-1} indicated the presence of the functional groups –OH and –COOH. Compared with the spectrum shown in Fig. 2-2, new adsorption peaks at 3196, 1516, 1429, and 1157 cm^{-1} can be found in the IR spectrum of PMIM/MWNTs (Fig. 2-3), which can be identified as the characteristic peaks of the polymer of the monomer and the cross-linker, similar to those shown in Fig. 2-4. This result supported that the polymer had been grafted to the surfaces of the MWNTs.

3.4. SEM images of PMIM/MWNTs

The SEM images of acid processed MWNTs and PMIM/MWNTs are shown in Fig. 3. In Fig. 3a, it can be seen that the acid processed MWNTs, which were used as supports for the PMIM/MWNTs, exhibited nanotube morphology with a high yield. Their average diameter was approximately 50 nm, and their lengths ranged from 5 to 15 μm. High magnification SEM images of the PMIM/MWNTs obtained are given in Fig. 3b. It can be seen that the diameters of the PMIM/MWNTs are generally larger than those of the acid processed MWNTs, indicating that the polymer was formed on the surface of the MWNTs. In Fig. 3c, a number of crumpled sites are evident on the surface of the PMIM/MWNTs, which provide more sites for binding with BSA. In addition, agglomeration of the polymer could be seen, which further supports the formation of the PMIM/MWNTs.

3.5. Adsorption isotherms and kinetics

Based on the above supposition concerning the effects of BSA concentration on its adsorption, this was investigated using both PMIM/MWNTs and nPMIM/MWNTs. The BSA equilibrium concentration, which depended on the amount of BSA adsorbed to the PMIM/MWNTs or nPMIM/MWNTs, is shown in Fig. 4-1 and -2. As can be seen, no difference in the adsorbance *Q* of BSA for PMIM/MWNTs and nPMIM/MWNTs could be observed when the BSA concentration was less than 0.01 mg/mL, while an obvious difference could be found when the concentration of BSA was above 0.1 mg/mL. It might be that the different adsorbance *Q* of BSA between PMIM/MWNTs and nPMIM/MWNTs was caused by the different quantity of available binding sites. At lower BSA concentration, the BSA quantity was not enough to saturate all

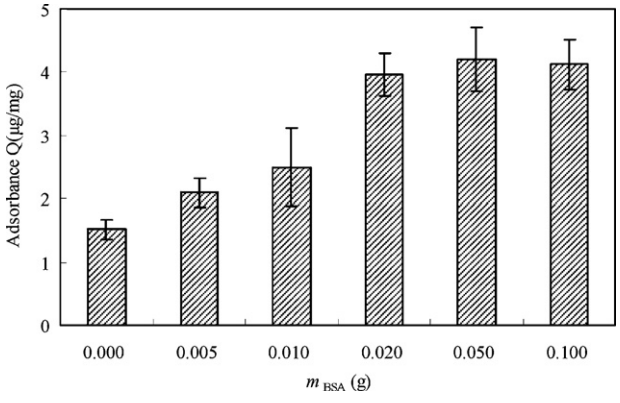

Fig. 1. Effect of the amount of BSA on the adsorption amount of the PMIM/MWNTs. The amount of other materials: 0.1 g of MWNTs; 0.24 g of AAm; 0.1 g of MBA.

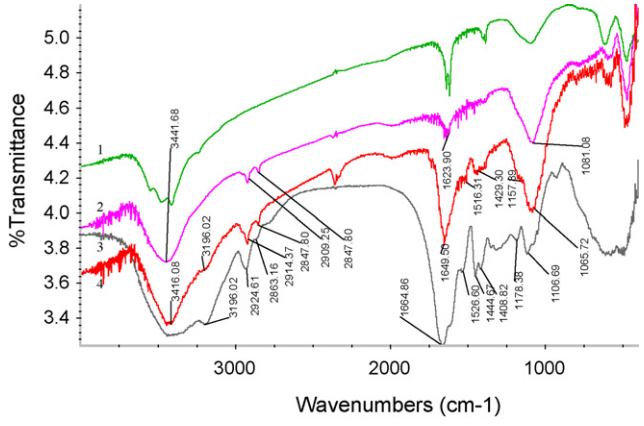

Fig. 2. FTIR spectra. (1) Received-MWNTs; (2) acid processed MWNTs; (3) PMIM/MWNTs; (4) polymer of monomer and cross-linker.

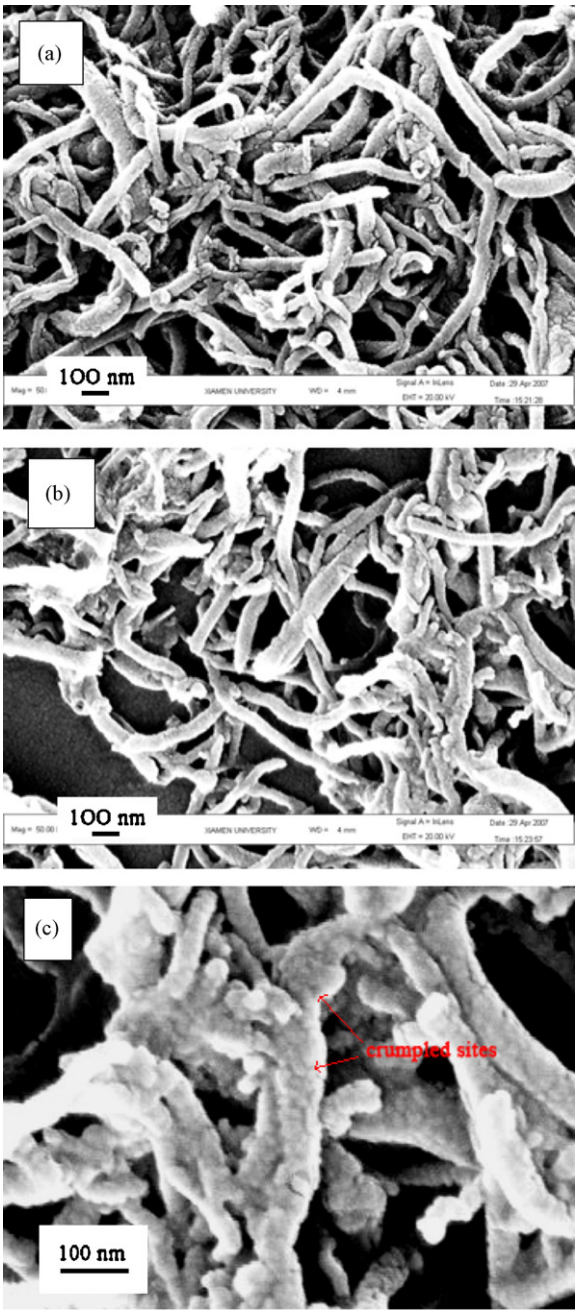

Fig. 3. SEM images of the acid processed MWNTs and PMIM/MWNTs. (a) The acid processed MWNTs; (b and c) PMIM/MWNTs.

the unspecific binding on the surfaces of the PMIM/MWNTs or nPMIM/MWNTs, resulting in no difference in their adsorbance. However, when BSA was saturated, the presence of specific binding cavities on the PMIM/MWNTs became evident. Furthermore, the adsorbance *Q* increased with increasing concentration of BSA, and a saturation value was achieved at a BSA concentration of 0.2 mg/mL, which represented saturation of the active binding cavities on the PMIM/MWNTs. Maximum adsorption capacity was 5.53 μg/mg PMIM/MWNTs. The results showed that PMIM/MWNTs have a higher binding capacity for BSA than that of nPMIM/MWNTs (1.82 μg/mg), comparing the adsorbance of molecularly imprinted polymers of standard dimensions in the literature [7,27,28], the PMIM/MWNTs exhibited excellent recognition and selective ability to BSA because of their high specific surface area and the unique characteristics of the nanomaterials.

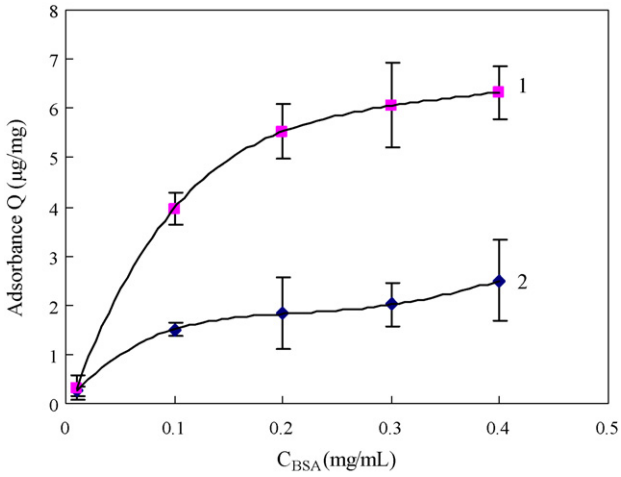

Fig. 4. Adsorption isotherms of PMIM/MWNTs (curve 1) and nPMIM/MWNTs (curve 2) to BSA. Amounts of PMIM/MWNTs or nPMIM/MWNTs: 200 mg; volume of BSA: 3 mL; time of adsorption: 3 h; vibration frequency: 150 r/min; $n = 3$.

The adsorption kinetics process of BSA on PMIM/MWNTs and nPMIM/MWNTs was studied, and the results are shown in Fig. 5. It can be clearly observed that the adsorbance *Q* of BSA increased with time and that a higher amount was absorbed by PMIM/MWNTs compared to nPMIM/MWNTs. The adsorption kinetics data showed that the adsorption rate was fastest in the first 5 h and that equilibrium was reached in 10 h.

3.6. Selectivity experiments

The crucial experiments for determining the selectivity of PMIM/MWNTs are the selectivity adsorption experiments. In these experiments, the PMIM/MWNTs was also tested for the binding of HSA and HB, which have MWs and isoelectric points similar to BSA, and for the binding of pepsin and HRP, which differ greatly in dimension and charge. The amounts of their adsorption onto the PMIM/MWNTs and nPMIM/MWNTs were determined (Fig. 6). The expectation was that the PMIM/MWNTs, having recognition cavities of BSA, would have higher adsorption capacities for BSA than for other molecules. The PMIM/MWNTs displayed a 2.6-fold increase in affinity to BSA compared to the nPMIM/MWNTs. PMIM/MWNTs, on the other hand, did not exhibit any significant change in affinity to other molecules compared to the nPMIM/MWNTs. These experiments thus demonstrated that PMIM/MWNTs can be synthe-

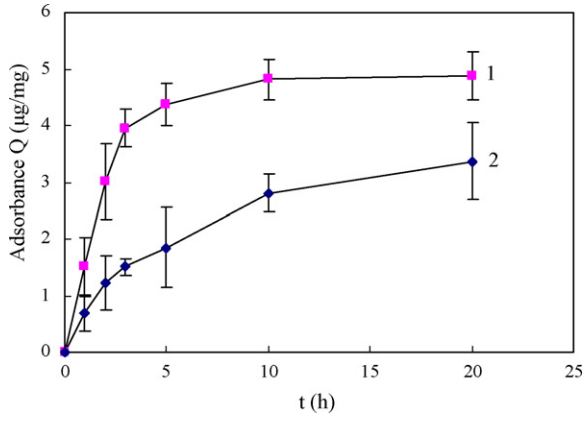

Fig. 5. Adsorption kinetics. The amounts of BSA adsorbed are plotted as the adsorption time, onto PMIM/MWNTs (curve 1) and nPMIM/MWNTs (curve 2). Amounts of wet PMIM/MWNTs or nPMIM/MWNTs: 200 mg; volume of BSA (100 μg/mL): 3 mL; time of absorption: 3 h; vibration frequency: 150 r/min; $n = 3$.

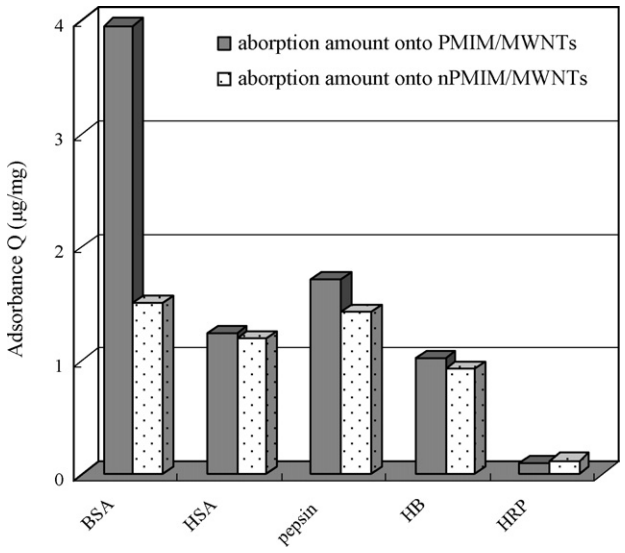

Fig. 6. Adsorption capacities of PMIM/MWNTs and nPMIM/MWNTs for BSA and similar molecules. Amounts of wet PMIM/MWNTs or nPMIM/MWNTs: 200 mg; concentration of analytes:100 μg/mL; time of absorption: 3 h; vibration frequency: 150 r/min.

sized which are selective to BSA based on shape selective cavities within the polymer, and so the PMIM/MWNTs are more selective to BSA than nPMIM/MWNTs because the imprinting methods create a microenvironment based on shape of cavity and size and positions of functional groups which recognize the imprinting molecule BSA.

4. Conclusions

The results presented here represent a further achievement in the area of protein imprinting. PMIM/MWNTs were synthesized using surface MIT on the surface of MWNTs, with BSA as a template molecule, AAm as the functional monomer, MBA as the cross-linker and $(NH_4)_2S_2O_8$ as the initiator. The amount of raw materials were: 0.1 g of MWNTs, 0.02 g of BSA, 0.24 g of AAm, 0.1 g of NNMBA and 0.025 mg of $(NH_4)_2S_2O_8$. The PMIM/MWNTs show a higher binding capacity for BSA than did the nPMIM/MWNTs. Maximum adsorption capacity was 5.53 μg/mg PMIM/MWNTs and a saturation value was achieved at a BSA concentration of 0.2 mg/mL. The selectivity adsorption experiments showed that the PMIM/MWNTs also had higher adsorption capacities for BSA than for such molecules, as HSA, HB, pepsin and HRP. The PMIM/MWNTs displayed a 2.6-fold increase in affinity to BSA compared to the nPMIM/MWNTs. The PMIM/MWNTs, on the other hand, did not exhibit any significant change in affinity to other molecules compared to the nPMIM/MWNTs.

Acknowledgements

This research was financially supported by the Program for Science and Technology Projects of the Education Department, Fujian Province of China (No. JA07165) and the National Nature Scientific Foundation of China (NSFC, No. 20775064), which are gratefully acknowledged. We express our sincere thanks to Professor John Hodgkiss of The University of Hong Kong for his assistance with English.

References

[1] G. Vlatakis, L.I. Andersson, R. Müller, K. Mosbach, Nature 361 (1993) 645.
[2] Y. Chen, M. Kele, P. Sajonz, B. Sellergren, G. Guiochon, Anal. Chem. 71 (1999) 928.
[3] A.G. Mayes, K. Mosbach, Anal. Chem. 68 (1996) 3769.
[4] M. Kempe, K. Mosbach, J. Chromatogr. A 691 (1995) 317.
[5] A. Bossi, S.A. Piletsky, E.V. Piletska, P.G. Righetti, A.P.F. Turner, Anal. Chem. 73 (2001) 5281.
[6] A. Bossi, F. Bonini, A.P.F. Turner, S.A. Piletsky, Biosens. Bioelectron. 22 (2007) 1131.
[7] F. Bonini, S. Piletsky, A.P.F. Turner, A. Speghini, A. Bossi, Biosens. Bioelectron. 22 (2007) 2322.
[8] N. Bereli, M. Andac, G. Baydemir, R. Say, I.Y. Galaev, A. Denizli, J. Chromatogr. A 1190 (2008) 18.
[9] S.C. Zimmerman, M.S. Wendland, N.A. Rakow, I. Zharov, K.S. Suslick, Nature 418 (2002) 399.
[10] C.D. Ki, C. Oh, S.G. Oh, J.Y. Chang, J. Am. Chem. Soc. 124 (2002) 14838.
[11] R.H. Schmidt, K. Mosbach, K. Haupt, Adv. Mater. 16 (2004) 719.
[12] M.M. Titirici, B. Sellergren, Chem. Mater. 18 (2006) 1773.
[13] M.A. Markowitz, P.R. Kust, G. Deng, P.E. Schoen, J.S. Dordick, D.S. Clerk, B.P. Gaber, Langmuir 16 (2000) 1759.
[14] D.M. Gao, Z.P. Zhang, M.H. Wu, C.G. Xie, G.J. Guan, D.P. Wang, J. Am. Chem. Soc. 129 (2007) 7859.
[15] C.G. Xie, Z.P. Zhang, D.P. Wang, G.J. Guan, D.M. Gao, J.H. Liu, Anal. Chem. 78 (2006) 8339.
[16] H.H. Yang, S.Q. Zhang, F. Tan, Z.X. Zhuang, X.R. Wang, J. Am. Chem. Soc. 127 (2005) 1378.
[17] Y. Li, H.H. Yang, Q.H. You, Z.X. Zhuang, X.R. Wang, Anal. Chem. 78 (2006) 317.
[18] S.Q. Zhang, H.H. Yang, Z.X. Zhuang, X.R. Wang, Chem. J. Chin. Univ. 25 (2004) 1028.
[19] Y. Li, X.F. Yin, F.R. Chen, H.H. Yang, Z.X. Zhuang, X.R. Wang, Macromolecules 39 (2006) 4497.
[20] C.D. Ki, J.Y. Chang, Macromolecules 39 (2006) 3415.
[21] Z. Li, J.F. Ding, M. Day, Y. Tao, Macromolecules 39 (2006) 2629.
[22] J.C.C. Yu, E.P.C. Lai, Polymer 66 (2006) 702.
[23] I.S. Chronakis, A. Jakob, B. Hagstrom, L. Ye, Langmuir 22 (2006) 8960.
[24] X.W. Kan, Y. Zhao, Z.R. Geng, Z.L. Wang, J.J. Zhu, J. Phys. Chem. C 112 (2008) 4849.
[25] C.G. Xie, B.H. Liu, Z.Y. Wang, D.M. Gao, G.J. Guan, Z.P. Zhang, Anal. Chem. 80 (2008) 437.
[26] J. Liu, A.G. Rinzler, H.J. Dai, J.H. Hafner, R.K. Bradley, P.J. Boul, A. Lu, T. Iverson, K. Shelimov, C.B. Huffman, F. Rodriguez-Macias, Y.S. Shon, T.R. Lee, D.T. Colbert, R.E. Smalley, Science 280 (1998) 1253.
[27] T.Y. Guo, Y.Q. Xia, G.J. Hao, B.H. Zhang, G.Q. Fu, Z. Yuan, B.L. He, J.F. Kennedy, Carbohydr. Polym. 62 (2005) 214.
[28] T.Y. Guo, Y.Q. Xia, J. Wang, M.D. Song, B.H. Zhang, Biomaterials 26 (2005) 5737.